THE LANCET
Infectious Diseases

Supplementary appendix

This appendix formed part of the original submission and has been peer reviewed. We post it as supplied by the authors.

Supplement to: Hoffmann M, Behrens GMN, Arora P, et al. Effect of hybrid immunity and bivalent booster vaccination on omicron sublineage neutralisation. *Lancet Infect Dis* 2022; published online Dec 5. https://doi.org/10.1016/S1473-3099(22)00792-7.

Appendix

Omicron sublineage-specific neutralisation activity elicited upon triple vaccination, breakthrough infection, and monovalent or bivalent vaccine boosters

Content

Table 1

Table 1: Plasma information

Cohort	ID	Gender	Age (years)	V1/V2/V3	Post V3 BTI (yes/no)	V4	Post V4 BTI (yes/no)	Time between sampling and last vaccination (days)	Time between sampling and positive PCR test last vaccination (days)	Anti-SARS-CoV-2 S1 IgG (BAU/ml)
V1/V2/V3[a]	7423	Male	33	BNT/BNT/BNT	no	no	no	19	n.a.	6019
	7531	Female	27	BNT/BNT/BNT	no	no	no	14	n.a.	3466
	7543	Female	53	BNT/BNT/BNT	no	no	no	41	n.a.	4243
	7551	Male	59	BNT/BNT/BNT	no	no	no	13	n.a.	4297
	7855	Female	38	AZ/BNT/BNT	no	no	no	14	n.a.	6963
	7857	Male	51	AZ/BNT/BNT	no	no	no	14	n.a.	3287
	7863	Female	38	AZ/BNT/BNT	no	no	no	14	n.a.	4836
	7866	Female	59	AZ/BNT/BNT	no	no	no	14	n.a.	7420
	7871	Male	42	AZ/AZ/BNT	no	no	no	14	n.a.	5483
	7884	Female	34	BNT/BNT/BNT	no	no	no	39	n.a.	4577
	7911	Female	54	AZ/BNT/BNT	no	no	no	14	n.a.	5021
	7938	Female	53	AZ/BNT/BNT	no	no	no	16	n.a.	5191
	7960	Male	39	BNT/BNT/BNT	no	no	no	24	n.a.	4202
	7973	Female	53	BNT/BNT/BNT	no	no	no	24	n.a.	6003
	7974	Female	59	BNT/BNT/BNT	no	no	no	45	n.a.	4077
	8051	Female	56	BNT/BNT/BNT	no	no	no	14	n.a.	3048
V1/V2/V3 + BTI(BA.1/BA.2)	8601	Female	43	BNT/BNT/BNT	yes (BA.1/2 wave)	no	no	102	31	4233
	8628	Female	38	AZ/BNT/BNT	yes (BA.1/2 wave)	no	no	123	48	7211
	8650	Female	38	AZ/BNT/BNT	yes (BA.1/2 wave)	no	no	128	14	2046
	8651	Female	35	AZ/BNT/BNT	yes (BA.1/2 wave)	no	no	128	23	1713
	8667	Female	50	AZ/AZ/BNT	yes (BA.1/2 wave)	no	no	118	13	4072
	8668	Female	40	BNT/BNT/BNT	yes (BA.1/2 wave)	no	no	140	56	4166
	8669	Female	22	AZ/BNT/BNT	yes (BA.1/2 wave)	no	no	132	36	5048
	8694	Male	46	BNT/BNT/BNT	yes (BA.1/2 wave)	no	no	131	8	3824
	8704	Female	39	AZ/BNT/BNT	yes (BA.1/2 wave)	no	no	128	24	5395
	8706	Male	30	AZ/BNT/BNT	yes (BA.1/2 wave)	no	no	134	30	7323
	8711	Female	30	AZ/BNT/BNT	yes (BA.1/2 wave)	no	no	128	21	9077

	8712	Female	39	AZ/BNT/BNT	yes (BA.1/2 wave)	no	no	134	59	2440
	8717	Female	38	AZ/BNT/BNT	yes (BA.1/2 wave)	no	no	136	31	2970
	8720	Female	35	AZ/BNT/BNT	yes (BA.1/2 wave)	no	no	136	31	2365
	8745	Female	41	BNT/BNT/BNT	yes (BA.1/2 wave)	no	no	173	62	1822
	8754	Male	36	AZ/BNT/BNT	yes (BA.1/2 wave)	no	no	164	44	3399
	8780	Male	38	AZ/BNT/BNT	yes (BA.1/2 wave)	no	no	144	31	9237
V1/V2/V3 + BTI(BA.5)	9004	Male	36	BNT/BNT/MOD	yes (BA.5 wave)	no	no	223	25	6567
	9027	Female	24	AZ/BNT/BNT	yes (BA.5 wave)	no	no	219	10	4662
	9029	Female	29	BNT/BNT/BNT	yes (BA.5 wave)	no	no	214	22	6618
	9061	Female	55	AZ/AZ/BNT	yes (BA.5 wave)	no	no	263	31	5452
	9063	Female	62	AZ/BNT/BNT	yes (BA.5 wave)	no	no	273	41	4891
	9071	Female	46	AZ/AZ/MOD	yes (BA.5 wave)	no	no	249	49	5499
	9072	Female	31	AZ/BNT/BNT	yes (BA.5 wave)	no	no	274	36	2392
	9092	Male	43	AZ/BNT/BNT	yes (BA.5 wave)	no	no	261	16	5495
	9099	Female	39	AZ/AZ/BNT	yes (BA.5 wave)	no	no	279	33	6023
	9108	Female	53	BNT/BNT/MOD	yes (BA.5 wave)	no	no	253	15	4515
	9112	Female	53	BNT/BNT/BNT	yes (BA.5 wave)	no	no	280	31	6801
	9142	Female	34	AZ/BNT/BNT	yes (BA.5 wave)	no	no	284	53	2922
	9144	Female	50	AZ/AZ/MOD	yes (BA.5 wave)	no	no	275	31	7392
	9145	Female	37	BNT/BNT/MOD	yes (BA.5 wave)	no	no	249	31	4194
	9166	Female	34	BNT/BNT/BNT	yes (BA.5 wave)	no	no	152	40	6810
	9189	Male	63	BNT/BNT/BNT	yes (BA.5 wave)	no	no	316	27	6661
	9202	Female	35	BNT/BNT/BNT	yes (BA.5 wave)	no	no	252	59	4818

	9232	Male	38	BNT/BNT/BNT	yes (BA.5 wave)	no	no	275	58	6338
	9238	Female	51	BNT/BNT/BNT	yes (BA.5 wave)	no	no	192	28	4170
	9247	Female	48	BNT/BNT/BNT	yes (BA.5 wave)	no	no	291	52	4974
	9271	Female	43	BNT/BNT/BNT	yes (BA.5 wave)	no	no	292	12	2768
	9290	Female	28	BNT/BNT/BNT	yes (BA.5 wave)	no	no	266	16	2557
	9297	Female	36	BNT/BNT/BNT	yes (BA.5 wave)	no	no	287	11	3551
	9316	Female	31	AZ/BNT/BNT	yes (BA.5 wave)	no	no	230	59	1602
	9334	Male	51	BNT/BNT/BNT	yes (BA.5 wave)	no	no	324	23	4845
	9335	Female	26	BNT/BNT/BNT	yes (BA.5 wave)	no	no	324	57	6751
	9358	Female	36	BNT/BNT/MOD	yes (BA.5 wave)	no	no	279	47	7600
V1/V2/V3/V4$_{monovalent}$[a]	8221	Male	48	AZ/AZ/BNT	no	yes (BNT)	no	30	n.a.	1826
	8380	Male	49	AZ/BNT/BNT	no	yes (BNT)	no	42	n.a.	2022
	8383	Male	44	BNT/BNT/BNT	no	yes (BNT)	no	37	n.a.	8018
	8391	Female	38	BNT/BNT/BNT	no	yes (BNT)	no	40	n.a.	2341
	8808	Female	59	AZ/BNT/BNT	no	yes (BNT)	no	7	n.a.	4709
	8830	Male	65	AZ/AZ/BNT	no	yes (BNT)	no	9	n.a.	1931
	8864	Female	49	BNT/BNT/BNT	no	yes (BNT)	no	46	n.a.	7836
	9292	Female	31	BNT/BNT/BNT	no	yes (BNT)	no	51	n.a.	5424
	9310	Male	53	BNT/BNT/BNT	no	yes (BNT)	no	2	n.a.	4990
	9351	Female	27	BNT/BNT/BNT	no	yes (BNT)	no	29	n.a.	11368
	9357	Female	58	BNT/BNT/BNT	no	yes (BNT)	no	33	n.a.	1668
V1/V2/V3/V4$_{monovalent}$ + BTI(BA.5)	8973	Female	30	BNT/BNT/MOD	no	yes (BNT)	yes (BA.5 wave)	85	8	3104
	9178	Female	29	BNT/BNT/BNT	no	yes (BNT)	yes (BA.5 wave)	148	60	1596
	9308	Female	38	BNT/BNT/BNT	no	yes (BNT)	yes (BA.5 wave)	230	44	1852
	9314	Male	31	BNT/BNT/BNT	no	yes (BNT)	yes (BA.5 wave)	143	30	12250
	9318	Male	49	AZ/BNT/BNT	no	yes (BNT)	yes (BA.5 wave)	232	35	6341
	9326	Male	59	BNT/BNT/BNT	no	yes (BNT)	yes (BA.5 wave)	107	48	9730

	9349	Female	55	BNT/BNT/BNT	no	yes (BNT)	yes (BA.5 wave)	83	15	5474
	9354	Female	43	BNT/BNT/BNT	no	yes (BNT)	yes (BA.5 wave)	181	45	9082
V1/V2/V3/V4$_{bivalent}$[a]	9387	Female	59	BNT/BNT/BNT	no	yes (BNT$_{bivalent}$)	no	27	n.a.	6161
	9413	Female	38	BNT/BNT/BNT	no	yes (BNT$_{bivalent}$)	no	29	n.a.	3183
	9445	Male	65	AZ/AZ/BNT	no	yes (BNT$_{bivalent}$)	no	27	n.a.	7177
	9446	Female	61	BNT/BNT/BNT	no	yes (BNT$_{bivalent}$)	no	27	n.a.	5104
	9448	Female	56	BNT/BNT/BNT	no	yes (BNT$_{bivalent}$)	no	11	n.a.	7945
	9452	Male	44	no information	no	yes (BNT$_{bivalent}$)	no	27	n.a.	12697
	9472	Female	54	no information	no	yes (BNT$_{bivalent}$)	no	33	n.a.	2720
	9474	Female	54	no information	no	yes (BNT$_{bivalent}$)	no	33	n.a.	2629
	9476	Female	51	no information	no	yes (BNT$_{bivalent}$)	no	33	n.a.	5429
	9477	Male	52	no information	no	yes (BNT$_{bivalent}$)	no	33	n.a.	2374
	9479	Male	62	no information	no	yes (BNT$_{bivalent}$)	no	33	n.a.	5576
	9481	Female	58	no information	no	yes (BNT$_{bivalent}$)	no	23	n.a.	8758
	9484	Male	45	no information	no	yes (BNT$_{bivalent}$)	no	33	n.a.	7828
	9485	Male	68	no information	no	yes (BNT$_{bivalent}$)	no	26	n.a.	2639
	9486	Female	52	no information	no	yes (BNT$_{bivalent}$)	no	23	n.a.	8519
	9488	Male	54	no information	no	yes (BNT$_{bivalent}$)	no	26	n.a.	2644
	9491	Female	46	no information	no	yes (BNT$_{bivalent}$)	no	33	n.a.	4773
	9493	Female	61	no information	no	yes (BNT$_{bivalent}$)	no	28	n.a.	4819
	9494	Female	50	no information	no	yes (BNT$_{bivalent}$)	no	33	n.a.	3610
	9495	Male	54	no information	no	yes (BNT$_{bivalent}$)	no	33	n.a.	2862
	9496	Male	40	BNT/BNT/MOD	no	yes (BNT$_{bivalent}$)	no	33	n.a.	8194
V1/V2/V3 + BTI(BA.1/BA.2) + V4$_{bivalent}$	9447	Female	47	BNT/BNT/BNT	yes (BA.1/2 wave)	yes (BNT$_{bivalent}$)	no	25	222	6583
	9468	Female	48	no information	yes (BA.1/2 wave)	yes (BNT$_{bivalent}$)	no	33	155-185[b]	5231
	9469	Female	44	no information	yes (BA.1/2 wave)	yes (BNT$_{bivalent}$)	no	33	233	11589
	9470	Female	22	no information	yes (BA.1/2 wave)	yes (BNT$_{bivalent}$)	no	33	186-215[b]	5343
	9471	Male	40	no information	yes (BA.1/2 wave)	yes (BNT$_{bivalent}$)	no	33	247-274[b]	7462
	9473	Female	58	no information	yes (BA.1/2 wave)	yes (BNT$_{bivalent}$)	no	33	210	10400
	9478	Female	42	no information	yes (BA.1/2 wave)	yes (BNT$_{bivalent}$)	no	33	186-215[b]	6435
	9480	Male	54	no information	yes (BA.1/2 wave)	yes (BNT$_{bivalent}$)	no	14	186-215[b]	6435

	9490	**Male**	**49**	**no information**	**yes (BA.1/2 wave)**	**yes ($BNT_{bivalent}$)**	**no**	**26**	**247-274[b]**	**13795**
	9492	**Male**	**50**	**no information**	**yes (BA.1/2 wave)**	**yes ($BNT_{bivalent}$)**	**no**	**33**	**216-246[b]**	**8372**
	9497	**Female**	**50**	**no information**	**yes (BA.1/2 wave)**	**yes ($BNT_{bivalent}$)**	**no**	**33**	**104**	**15010**

[a]: SARS-CoV-2 infection-free status of V1/V2/V3, V1/V2/V3/$V4_{monovalent}$ and V1/V2/V3/$V4_{bivalent}$ cohorts was confirmed by ELISA (anti-NCP-negative).

[b]: Only the information of the month of positive PCR testing was available.

Abbreviations: AZ, AZD1222/Vaxzevria; BNT, BNT162b2/Comirnaty; MOD, mRNA-1273/Spikevax; $BNT_{bivalent}$, Comirnaty Original/Omicron BA.4-5; BAU, binding antibody units; BTI, breakthrough infection;

Table 2

Table 2: Cohort characteristics.

		Cohort						
		A	B	C	D	E	F	G
Participants (n)		16	17	27	11	8	21	10
Gender	Male (n)	5	4	5	5	3	9	4
	Male (%)	31.3	23.5	18.5	45.5	37.5	42.9	36.4
	Female (n)	11	13	22	6	5	12	7
	Female (%)	68.8	76.5	81.5	54.5	62.5	57.1	63.6
Age (years)	Median	52	38	38	49	40.5	54	48.5
	Range	27-59	22-50	24-63	27-65	29-59	38-68	40-58
	25%; 75% Percentile	38; 55.5	35; 40.5	34; 51	38; 58	30.3; 53.5	48; 60	43.5; 51
Time since last immunisation event (days)	Median	14	31	31	33	39.5	29	33
	Range	13-45	8-62	10-59	2-51	8-60	11-33	14-33
	25%; 75% Percentile	14; 24	22; 46	22; 49	9; 42	18.8; 47.3	26.5; 33	26; 33
Total SARS-CoV-2 B.1 S1 IgG (BAU/ml)	Median	4,707	4,072	4,974	4,709	5,908	5,104	7,462
	Range	3,048 - 7,420	1,713-9,237	1,602-7,600	1,668-11,368	1,596-12,250	2,374-12,697	5,431-15,010
	25%; 75% Percentile	4,108; 5,873	2,403; 6,303	4,170; 6,618	1,931; 7,836	2,165; 9,568	2,791; 7,887	6,435; 11,589

Cohorts: A, V1/V2/V3; B, V1/V2/V3 + BTI(BA.1/BA.2); C, V1/V2/V3 + BTI(BA.5); D, V1/V2/V3/$V4_{monovalent}$; E, V1/V2/V3/$V4_{monovalent}$ + BTI(BA.5); F, V1/V2/V3/$V4_{bivalent}$; G, V1/V2/V3 + BTI(BA.1/BA.2) + $V4_{bivalent}$.

Table 3

Table 3: Median fold change in NT50 versus B.1.

Cohort	Median Fold Change in NT50 vs. B.1 (95% CI)						
	B.1	BA.1	BA.4; BA.5	BA.4.6	BA.2.75.2	BJ.1	BQ.1.1
A	1,0x (1.0x; 1.0x)	-6,6x (-5.3x; -8.6x)	-20,2x (-13.1x; -28.4x)	-32,7x (-20.8x; -41.2x)	-573,0x (-47.2x; -1,426x)	-25,5x (-19.8x; -38.8x)	-103,2x (-60.8x; -1,029x)
B	1,0x (1.0x; 1.0x)	-2,6x (-2.0x; -4.2x)	-6,0x (-4.3x; -9.4x)	-8,8x (-6.0x; -15.8x)	-35,1x (-22.1x; -91.2x)	-12,9x (-7.9x; -18.6x)	-30,8x (-19.5x; -87.7x)
C	1,0x (1.0x; 1.0x)	-4,3x (-3.0x; -5.8x)	-4,0x (-3.2x; -4.5x)	-5,1x (-4.0x; -6.6x)	-36,9x (-28.3x; -42.3x)	-6,5x (-5.8x; -10.9x)	-22,7x (-16.3x; -27.6x)
D	1,0x (1.0x; 1.0x)	-7,1x (-4.1x; -8.7x)	-10,4x (-6.6x; -18.2x)	-16,7x (-10.5x; -30.7x)	-57,4x (-40.6x; -849x)	-10,9x (-8.0x; -23.4x)	-96,8x (-23.6x; -849x)
E	1,0x (1.0x; 1.0x)	-5,1x (-2.3x; -17.4x)	-5,6x (-2.2x; -20.9x)	-7,0x (-2.3x; -20.9x)	-54,0x (-18,7x; -824x)	-13,1x (-2.3x; -35.1x)	-31,5x (-16.2x; -1,652x)
F	1,0x (1.0x; 1.0x)	-3,4x (-2.7x; -4.9x)	-4,8x (-3.6x; -8.9x)	-9,6x (-5.1x; -11.9x)	-40,2x (-18.3x; -702x)	-6,2x (-4.2x; -9.2x)	-32,3x (-18.2x; -448x)
G	1,0x (1.0x; 1.0x)	-2,1x (-1.4x; -2.8x)	-3,0x (-2.1x; -4.6x)	-5,7x (-3.3x; -7.2x)	-17,4x (-9.2x; -30.5x)	-4,3x (-2.0x; -6.7x)	-11,7x (-8.1x; -22.9x)

Cohorts: A, V1/V2/V3; B, V1/V2/V3 + BTI(BA.1/BA.2); C, V1/V2/V3 + BTI(BA.5); D, V1/V2/V3/$V4_{monovalent}$; E, V1/V2/V3/$V4_{monovalent}$ + BTI(BA.5); F, V1/V2/V3/$V4_{bivalent}$; G, V1/V2/V3 + BTI(BA.1/BA.2) + $V4_{bivalent}$. Abbreviation: 95% CI, 95% confidence interval.

Table 4

Table 4: Median fold change in NT50 versus BA.4-5.

Cohort	Median Fold Change in NT50 vs. BA.4; BA.5 (95% CI)						
	B.1	BA.1	BA.4-5	BA.4.6	BA.2.75.2	BJ.1	BQ.1.1
A	+20,2x (+13.1x; +28.4x)	+3,0x (+2.1x; +3.9x)	1,0x (1.0x; 1.0x)	-1,6x (-1.5x; -1.7x)	-15,5x (-4.5x; -83.1x)	-1,4x (-1.9x; 1.0x)	-6,2x (-3.4x; -24.5x)
B	+6,0x (+4.3x; +9.4x)	+2,3x (+1.5x; +2.9x)	1,0x (1.0x; 1.0x)	-1,4x (-1.3x; -1.6x)	-4,6x (-3.7x; -13.3x)	-1,7x (-1.4x; -2.2x)	-4,6x (-3.3x; -10.6x)
C	+4,0x (+3.2x; +4.5x)	+1,0x (-1.4x; +1.2x)	1,0x (1.0x; 1.0x)	-1,3x (-1.2x; -1.5x)	-10,8x (-7.8x; -12.2x)	-2,2x (-1.5x; -2.9x)	-5,5x (-4.3x; -6.5x)
D	+10,4x (+6.6x; +18.2x)	+1,5x (1.0x; +2.6x)	1,0x (1.0x; 1.0x)	-1,6x (-1.3x; -2.5x)	-8,7x (-3.0x; -41.1x)	-1,0x (-2.2x; +1.3x)	-7,9x (-3.5x; -41.1x)
E	+5,6x (+2.2x; +20.9x)	+1,1x (-1.4x; +2.4x)	1,0x (1.0x; 1.0x)	-1,2x (-2.3x; +1.2x)	-9,9x (-6.0x; -39.5x)	-1,7x (-4.8x; +1.3x)	-8,2x (-2.6x; -357x)
F	+4,8x (+3.6x; +8.9x)	+1,4x (-1.1x; +1.6x)	1,0x (1.0x; 1.0x)	-1,6x (-1.3x; -1.8x)	-8,5x (-3.8x; -107x)	-1,3x (-1.7x; +1.1x)	-5,9x (-3.6x; -11.2x)
G	+3,0x (+2.1x; +4.6x)	+1,5x (+1.1; +2.8x)	1,0x (1.0x; 1.0x)	-1,6x (-2.1x; +1.1x)	-5,0x (-3.6x; -7.9x)	-1,2x (-1.9x; +1.1x)	-3,5x (-2.9x; -7.1x)

Cohorts: A, V1/V2/V3; B, V1/V2/V3 + BTI(BA.1/BA.2); C, V1/V2/V3 + BTI(BA.5); D, V1/V2/V3/$V4_{monovalent}$; E, V1/V2/V3/$V4_{monovalent}$ + BTI(BA.5); F, V1/V2/V3/$V4_{bivalent}$; G, V1/V2/V3 + BTI(BA.1/BA.2) + $V4_{bivalent}$. Abbreviation: 95% CI, 95% confidence interval.

Methods

Cell culture

Vero (African green monkey kidney, female, kidney; CRL-1586, ATCC; RRID: CVCL 0574, kindly provided by Andrea Maisner) and 293T cells (human, female, kidney; ACC-635, DSMZ; RRID: CVCL 0063) were cultured in Dulbecco's modified Eagle medium (PAN-Biotech), supplemented with 10% fetal bovine serum (Biochrom), 100 U/ml of penicillin, and 0.1 mg/ml of streptomycin (PAN-Biotech) at 37 °C in a humidified atmosphere containing 5% CO_2. Validation of cell lines was performed by STR analysis, partial sequencing of the cytochrome c oxidase gene, microscopic examination, and/or according to cell line-specific growth characteristics. Cell lines were routinely tested for mycoplasma contamination. 293T cells were transfected by calcium phosphate precipitation.

Expression plasmids and sequence analysis

Information on S protein sequences was retrieved from GISAID (Global Initiative on Sharing All Influenza Data) (https://gisaid.org/) and CoV-Spectrum (https://cov-spectrum.org/) databases. Expression plasmids pCAGGS-DsRed[1], pCG1-SARS-CoV-2 B.1 SΔ18 (codon-optimised, C-terminal truncation of 18 amino acid residues, GISAID Accession ID: EPI_ISL_425259)[2], pCG1-SARS-CoV-2 BA.1 SΔ18 (codon-optimised, C-terminal truncation of 18 amino acid residues, GISAID Accession ID: EPI_ISL_6640919)[3], pCG1-SARS-CoV-2 BA.4-5 SΔ18 (codon-optimised, C-terminal truncation of 18 amino acid residues, GISAID Accession ID: EPI_ISL_11550739 and EPI_ISL_12029894)[4] and pCG1-SARS-CoV-2 BA.4.6 SΔ18 (codon-optimised, C-terminal truncation of 18 amino acid residues, GISAID Accession ID: EPI_ISL_14429885)[5] have been described elsewhere. In addition, expression plasmids for SARS-CoV-2 BA.2.75.2 SΔ18 (GISAID Accession ID: EPI_ISL_15019960), SARS-CoV-2 BJ.1 SΔ18 (GISAID Accession ID: EPI_ISL_14913530) and SARS-CoV-2 BQ.1.1 SΔ18 (GISAID Accession ID: EPI_ISL_14752457) were generated by Gibson assembly. For this, overlapping DNA strings were synthesised (five strings for each S protein; Thermo Fisher Scientific, sequences available upon request). Gene strings and linearised (BamHI/XbaI digest) pCG1 plasmid (a kind gift of Roberto Cattaneo, Mayo Clinic College of Medicine, Rochester, MN, USA) were mixed with GeneArt™ Gibson Assembly HiFi Master Mix (Thermo Fisher Scientific) and the assembly was carried out according to manufacturer's

instructions. All S protein sequences were verified by Sanger sequencing using a commercial service (Microsynth SeqLab).

Pseudovirus particle production

Vesicular stomatitis virus pseudotype particles bearing SARS-CoV-2 S proteins were produced according to a published protocol[6]. 293T cells expressing the respective S protein or DsRed (negative control) upon transfection were inoculated with VSV-G-transcomplemented VSV*ΔG(FLuc) (kindly provided by Gert Zimmer)[7] at a multiplicity of infection of 3. The inoculum was removed after 1h of incubation and cells were washed with PBS and medium containing anti-VSV-G antibody (culture supernatant from I1-hybridoma cells; ATCC no. CRL-2700) was added. After 16-18h of incubation, cell culture supernatants were collected, clarified by centrifugation (4,000 x g, 10 min), and stored at -80 °C until further use.

Neutralisation assay

Neutralisation assays were performed in 96-well format according to a previously published protocol[8]. First, pseudotype particles bearing the respective S proteins were pre-incubated (30 min at 37°C) with different dilutions of heat-inactivated blood plasma (56 °C, 30 min), starting at a plasma dilution of either 1:25 or 1:50. Subsequently, the mixtures were added to confluent Vero cell layers. At 16–18 h postinoculation, the culture medium was aspirated and cells were lysed by incubation (30 min, room temperature) with PBS containing 0.5% Triton X-100 (Carl Roth). Next, lysates were transferred into white 96-well plates, and firefly luciferase substrate (Beetle-Juice, PJK) was added, before luminescence was recorded using a Hidex Sense plate luminometer (Hidex). Neutralisation efficiency was determined based on the relative inhibition of pseudovirus entry, using pseudovirus particles incubated in the absence of plasma as reference (= 0% inhibition). Samples that yielded an NT50 value lower than 6.25 (for samples with a starting dilution of 1:25) or 12.5 (for samples with a starting dilution of 1:50) were considered negative and were assigned an NT50 value of 1.

Ethics committee approval and enrolment of study participants

Collection of plasma samples was performed after approval by the research ethics committee of the Institutional Review Board of MHH (8973 BO K 2020). Each participant provided written informed

consent prior to the use of plasma samples for research. Participants for this analysis were from the COVID-19 Contact (CoCo) Study (German Clinical Trial Registry, DRKS00021152), which started in March 2020 and is an ongoing, prospective observational study monitoring anti-SARS-CoV-2 IgG and immune responses in health care professionals (HCP) at Hannover Medical School and individuals with potential contact to SARS-CoV-2[9,10]. Participants provide regularly blood samples for anti-Spike IgG and anti-nucleocapsid (NCP) IgG assessment. In addition, self-reported information about COVID-19 vaccinations and SARS-CoV-2 infection history including symptoms were collected via standardized questionnaires.

Plasma samples

All plasma samples were pre-screened for SARS-CoV-2 S1-specific IgG using the anti-SARS-CoV-2-QuantiVac-ELISA (IgG) (EUROIMMUN). A total of seven cohorts were tested. All plasma samples were collected within two months post vaccination/breakthrough infection (BTI); (i) cohort 1 (V1/V2/V3): individuals vaccinated with either one dose of AZD1222/Vaxzevria followed by two doses of BNT162b2/Comirnaty, two doses of AZD1222/Vaxzevria followed by one dose of BNT162b2/Comirnaty, or three doses of BNT162b2/Comirnaty (n = 16; median age = 52 years; male to female ratio 5:11); (ii) cohort 2 (V1/V2/V3 + $BTI_{BA.1/BA.2}$): individuals with a history of three vaccinations that experienced a BTI during the BA.1/BA.2 wave (January to May 2022 in Germany) (n = 17; median age = 38 years; male to female ratio 4:13); (iii) cohort 3 (V1/V2/V3 + $BTI_{BA.5}$): individuals with a history of three vaccinations that experienced a BTI during the BA.5 wave (June 2022 to present [November 2022] in Germany) (n = 27; median age = 38 years; male to female ratio 5:22); (iv) cohort 4 ($V1/V2/V3/V4_{monovalent}$): individuals that received a fourth vaccination with the monovalent BNT162b2/Comirnaty vaccine (n = 11; median age = 49 years; male to female ratio 5:6); (v) cohort 4 ($V1/V2/V3/V4_{monovalent}$ + $BTI_{BA.5}$): individuals that received a fourth vaccination with the monovalent BNT162b2/Comirnaty vaccine and experienced a BTI during the BA.5 wave (n = 8; median age = 40.5 years; male to female ratio 3:5); (vi) cohort 6 ($V1/V2/V3/V4_{bivalent}$): individuals that received a fourth vaccination with the B.1/BA.4-5 bivalent BNT162b2/Comirnaty Original/Omicron BA.4-5 vaccine (n = 21; median age = 54 years; male to female ratio 9:12); (vii) cohort 7 (V1/V2/V3 + $BTI_{BA.1/BA.2}$ + $V4_{bivalent}$): individuals with a history of three vaccinations that experienced a BTI during the BA.1/BA.2 wave and

later received a fourth vaccination with the B.1/BA.4-5 bivalent BNT162b2/Comirnaty Original/Omicron BA.4-5 vaccine (n = 11; median age = 48.5 years; male to female ratio 4:7). Individual information on the plasma samples can be found in the Appendix Table. SARS-CoV-2 infection-free history of V1/V2/V3, V1/V2/V3/$V4_{monovalent}$ and V1/V2/V3/$V4_{bivalent}$ cohorts was confirmed by absence of anti-SARS-CoV-2 NCP IgG using the anti-SARS-CoV-2 ELISA (NCP) (EUROIMMUN).

Data analysis

Data were analysed using Microsoft Excel (part of Microsoft Office Professional Plus, version 2016, Microsoft Corporation) and GraphPad Prism version 8.3.0 (GraphPad Software). Plasma dilutions leading to half-maximal inhibition (neutralising titre 50, NT50) were calculated using a non-linear regression model. Statistical significance was assessed by Wilcoxon matched-pairs signed rank test or Kruskal-Wallis analysis with Dunn's multiple comparisons test. Only p values of 0.05 or lower were considered statistically significant (ns [not significant], $p > 0.05$; *, $p \leq 0.05$; **, $p \leq 0.01$; ***, $p \leq 0.001$).

Limitations of the study

The following limitations apply to this study. First, neutralisation of SARS-CoV-2 was analysed using pseudotype particles bearing SARS-CoV-2 S protein, instead of authentic SARS-CoV-2 isolates, which were not available to us. While pseudovirus particles were shown to faithfully recapitulate host cell entry and neutralisation of ancestral SARS-CoV-2, our data await formal confirmation with clinical isolates of SARS-CoV-2 Omicron sublineages. Second, due to lack of donor-matched samples following V3 and $V4_{monovalent}$/$V4_{bivalent}$, we were only able to indirectly assess the impact of mono- and bivalent vaccine boosters on SARS-CoV-2 neutralisation. Third, we did not investigate the impact of B.1/BA.1-based bivalent booster vaccination on SARS-CoV-2 neutralisation following standard three-dose vaccination with or without BTI. Fourth, all plasma samples were collected within 2 months post vaccination/infection. As a consequence, we cannot formally rule out that differences in the relative neutralisation efficiency among SARS-CoV-2 lineages may change over time. Sixth, while this study assessed neutralising activity in seven cohorts with diverse immunisation histories, sample size for each cohort is relatively small and minor differences with respect to age exist among cohorts. Therefore, additional data is needed to confirm results in larger cohorts that may also allow for assessment of potential age and/or gender-related effects.

Acknowledgements

We gratefully acknowledge the originating laboratories responsible for obtaining the specimens, as well as the submitting laboratories where the genome data were generated and shared via GISAID, on which this research is based. We thank all study participants for their support and Janine Topal, Gema Morillas Ramos, Noemí Calderón Hampel and Metodi V. Stankov for technical and logistical help.

Supplementary references

1. Hoffmann M, Kleine-Weber H, Schroeder S, et al. SARS-CoV-2 Cell Entry Depends on ACE2 and TMPRSS2 and Is Blocked by a Clinically Proven Protease Inhibitor. *Cell* 2020; **181**(2): 271-80 e8.
2. Hoffmann M, Arora P, Gross R, et al. SARS-CoV-2 variants B.1.351 and P.1 escape from neutralizing antibodies. *Cell* 2021; **184**(9): 2384-93 e12.
3. Hoffmann M, Kruger N, Schulz S, et al. The Omicron variant is highly resistant against antibody-mediated neutralization: Implications for control of the COVID-19 pandemic. *Cell* 2022; **185**(3): 447-56 e11.
4. Arora P, Kempf A, Nehlmeier I, et al. Augmented neutralisation resistance of emerging omicron subvariants BA.2.12.1, BA.4, and BA.5. *Lancet Infect Dis* 2022; **22**(8): 1117-8.
5. Arora P, Zhang L, Nehlmeier I, et al. The effect of cilgavimab and neutralisation by vaccine-induced antibodies in emerging SARS-CoV-2 BA.4 and BA.5 sublineages. *The Lancet Infectious diseases* 2022.
6. Kleine-Weber H, Elzayat MT, Wang L, et al. Mutations in the Spike Protein of Middle East Respiratory Syndrome Coronavirus Transmitted in Korea Increase Resistance to Antibody-Mediated Neutralization. *J Virol* 2019; **93**(2).
7. Berger Rentsch M, Zimmer G. A vesicular stomatitis virus replicon-based bioassay for the rapid and sensitive determination of multi-species type I interferon. *PLoS One* 2011; **6**(10): e25858.
8. Arora P, Zhang L, Rocha C, et al. Comparable neutralisation evasion of SARS-CoV-2 omicron subvariants BA.1, BA.2, and BA.3. *The Lancet Infectious diseases* 2022; **22**(6): 766-7.
9. Barros-Martins J, Hammerschmidt SI, Cossmann A, et al. Immune responses against SARS-CoV-2 variants after heterologous and homologous ChAdOx1 nCoV-19/BNT162b2 vaccination. *Nat Med* 2021; **27**(9): 1525-9.
10. Behrens GMN, Cossmann A, Stankov MV, et al. Strategic Anti-SARS-CoV-2 Serology Testing in a Low Prevalence Setting: The COVID-19 Contact (CoCo) Study in Healthcare Professionals. *Infect Dis Ther* 2020; **9**(4): 837-49.

Supplementary figures

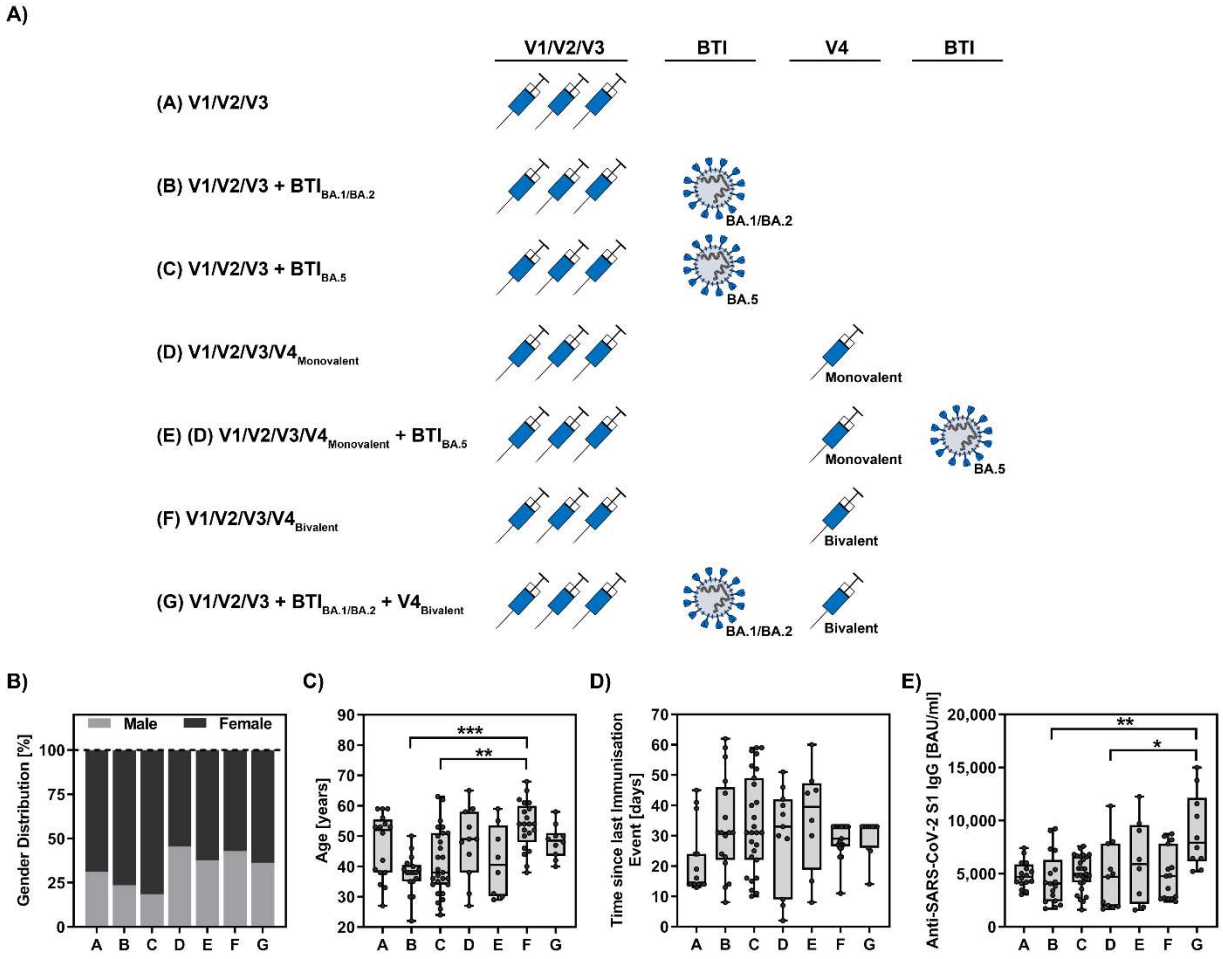

Figure S1: Comparison of the cohorts.

Schematic overview on the immunisation histories of the different cohorts (A) and comparison of cohorts regarding gender distribution (B), age (C), time between the last immunisation event and sampling (D), and total SARS-CoV-2 B.1 S1 IgG (E). Panels C-E: Box plots show median (black line) and 25%/75% quartiles, while bars indicate the range (circles represent individual samples). Statistical significance was assessed by Kruskal-Wallis analysis with Dunn's multiple comparisons test (not significant, $p > 0.05$; *, $p \leq 0.05$; **, $p \leq 0.01$; ***, $p \leq 0.001$; only data pairs with p values of 0.05 or lower are indicated).

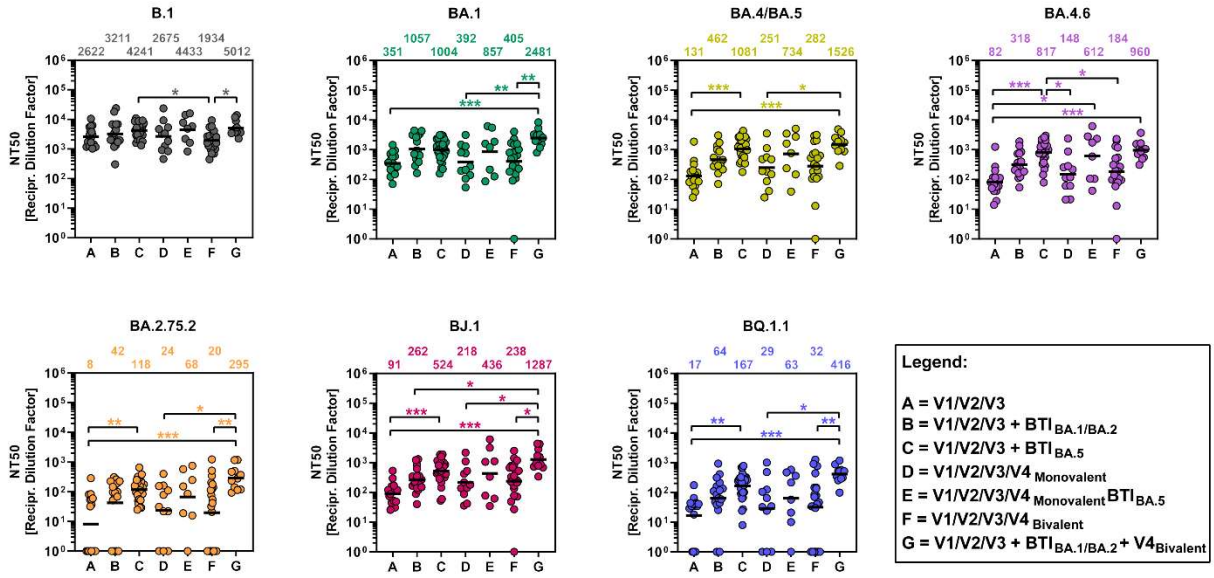

Figure S2: Neutralisation efficiency of SARS-CoV-2 lineages.

The data on neutralisation efficiency were re-grouped according to the respective SARS-CoV-2 lineage.

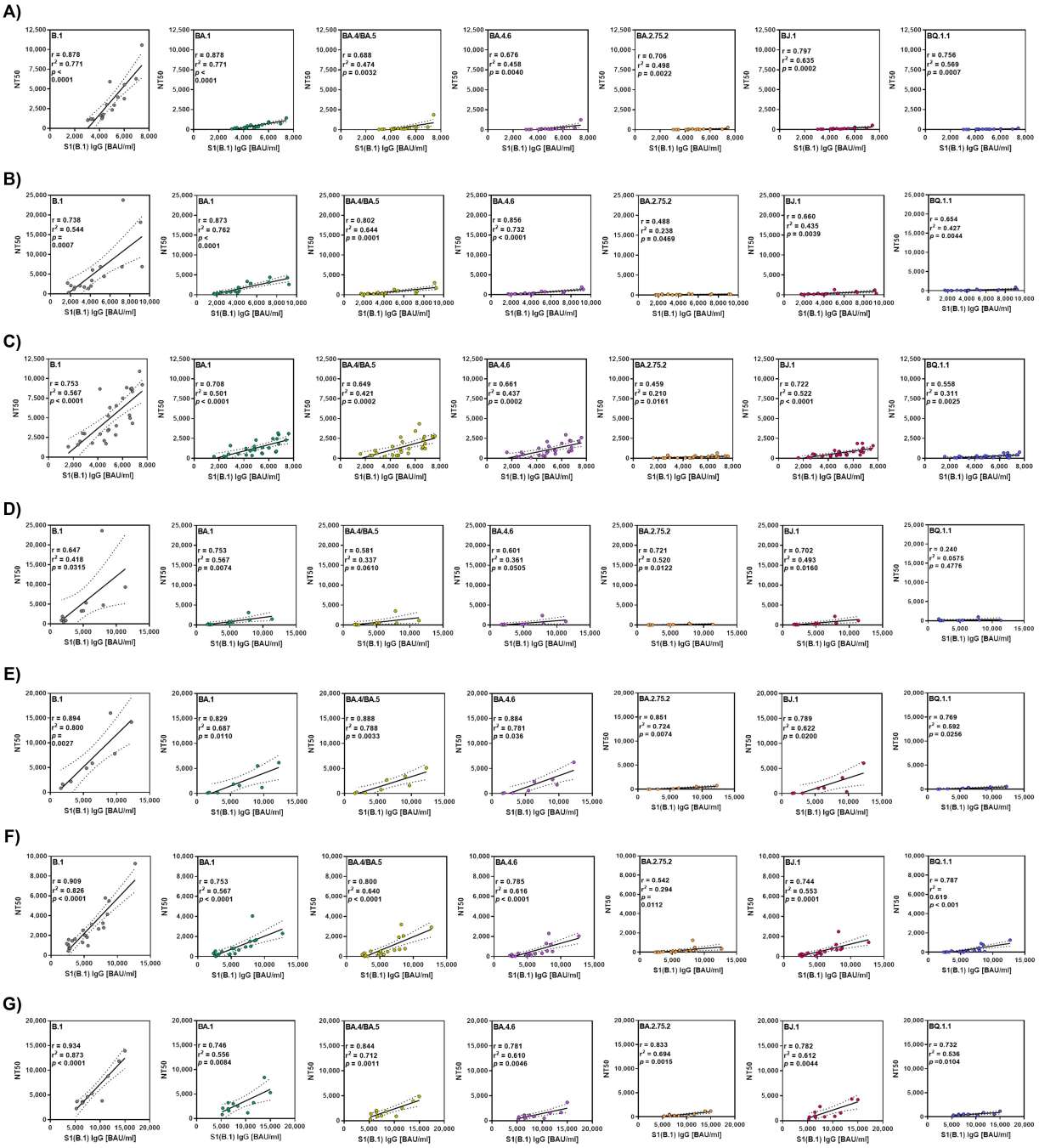

Figure S3: Correlation of total SARS-CoV-2 B.1 S1 IgG and lineage-specific neutralisation activity.

Total SARS-CoV-2 B.1 S1 IgG (given as BAU/ml) were quantified by ELISA and correlated with neutralisation activity against pseudoviruses bearing the S proteins of the indicated SARS-CoV-2 lineages. Cohorts:

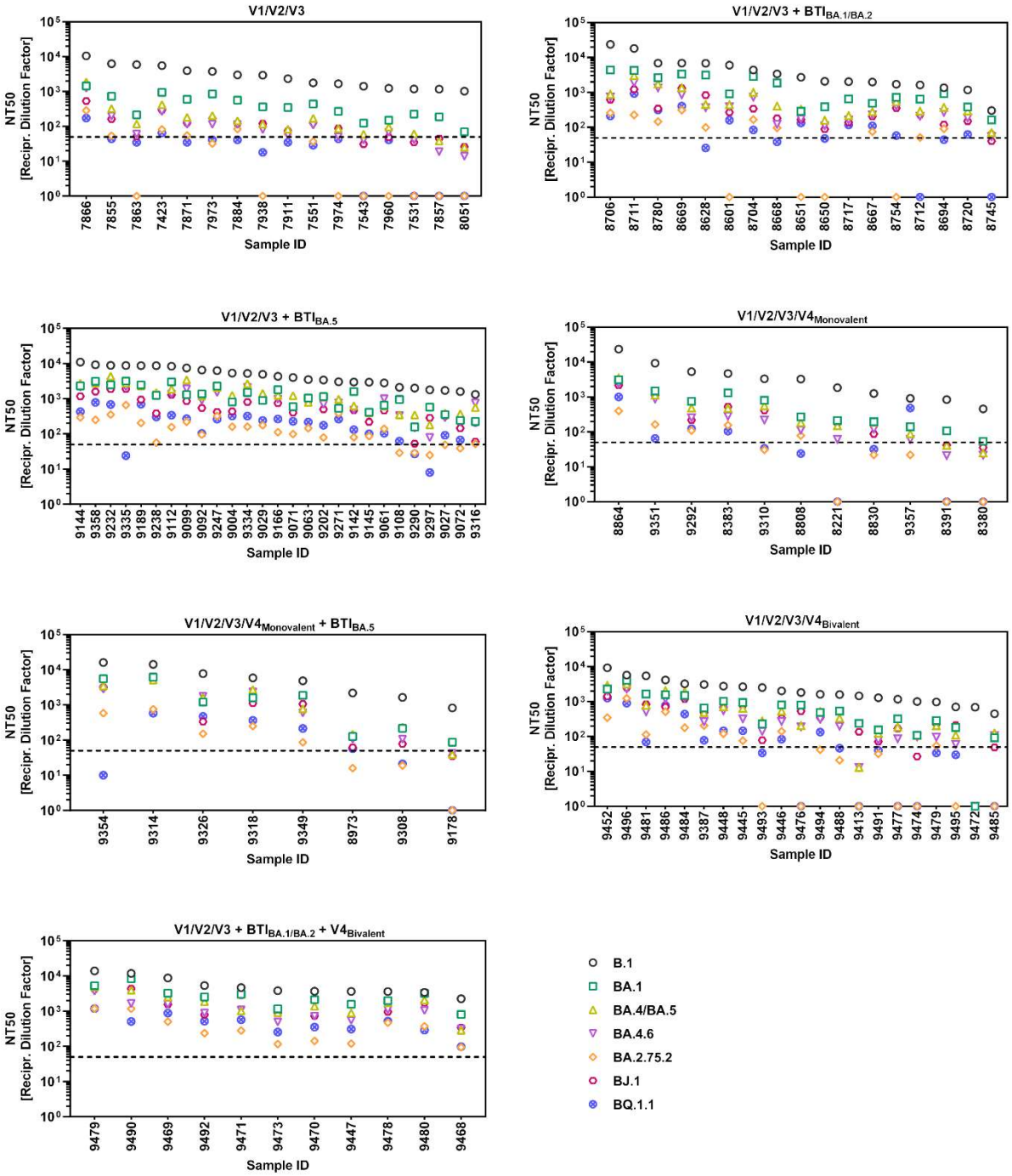

Figure S4: Individual neutralisation data ranked according to B.1 neutralisation.

Individual neutralisation data were ranked according to NT50 values for B.1 (from highest to lowest).

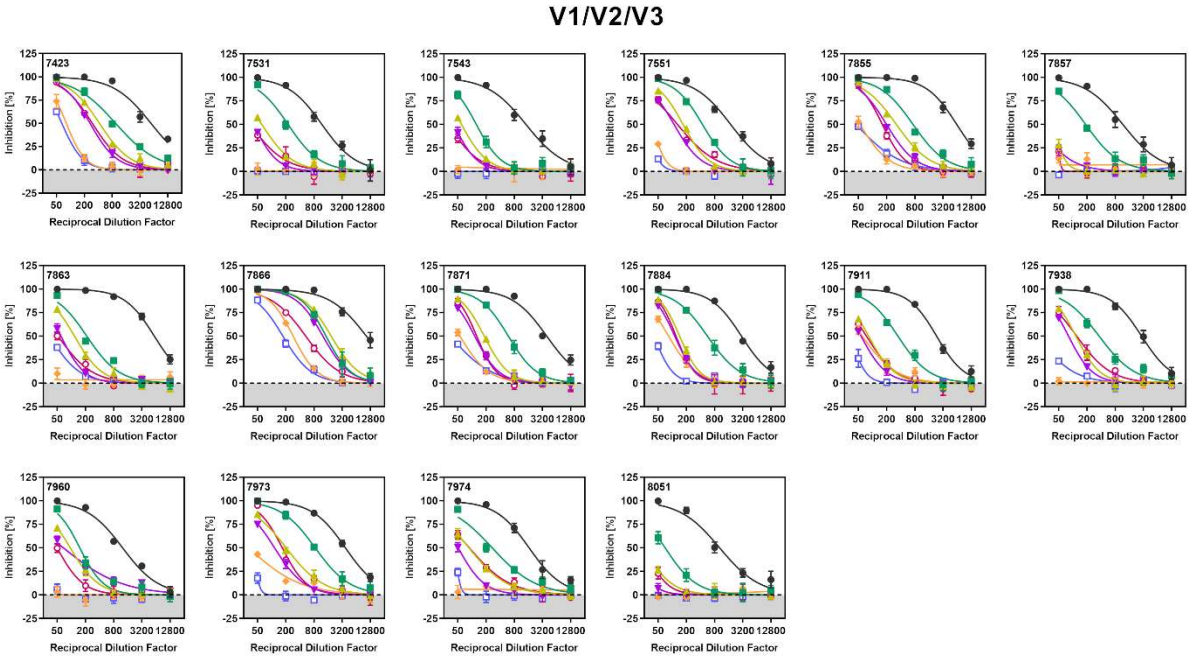

Figure S5: Individual neutralisation data for cohort V1/V2/V3.

Plasma-specific neutralisation data for SARS-CoV-2 lineages B.1 (dark grey), BA.1 (green), BA.4-5 (yellow), BA.4.6 (purple), BA.2.75.2 (orange), BJ.1 (pink), and BQ.1.1 (blue).

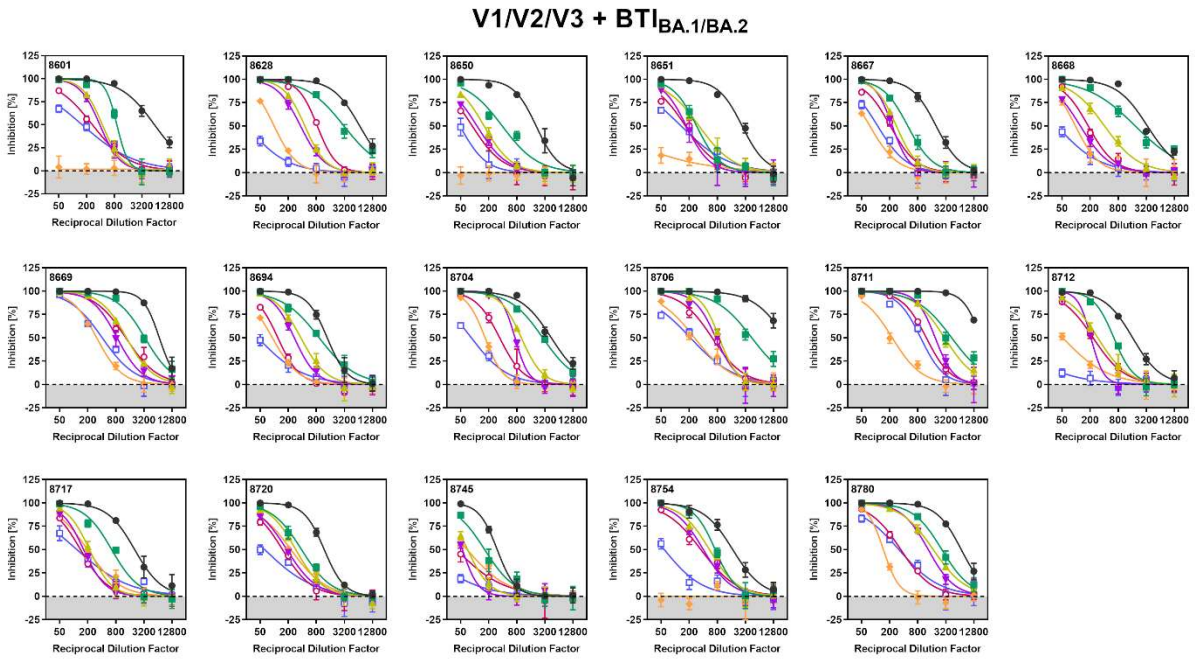

Figure S6: Individual neutralisation data for cohort V1/V2/V3 + BTI$_{BA.1/BA.2}$.

Plasma-specific neutralisation data for SARS-CoV-2 lineages B.1 (dark grey), BA.1 (green), BA.4-5 (yellow), BA.4.6 (purple), BA.2.75.2 (orange), BJ.1 (pink), and BQ.1.1 (blue).

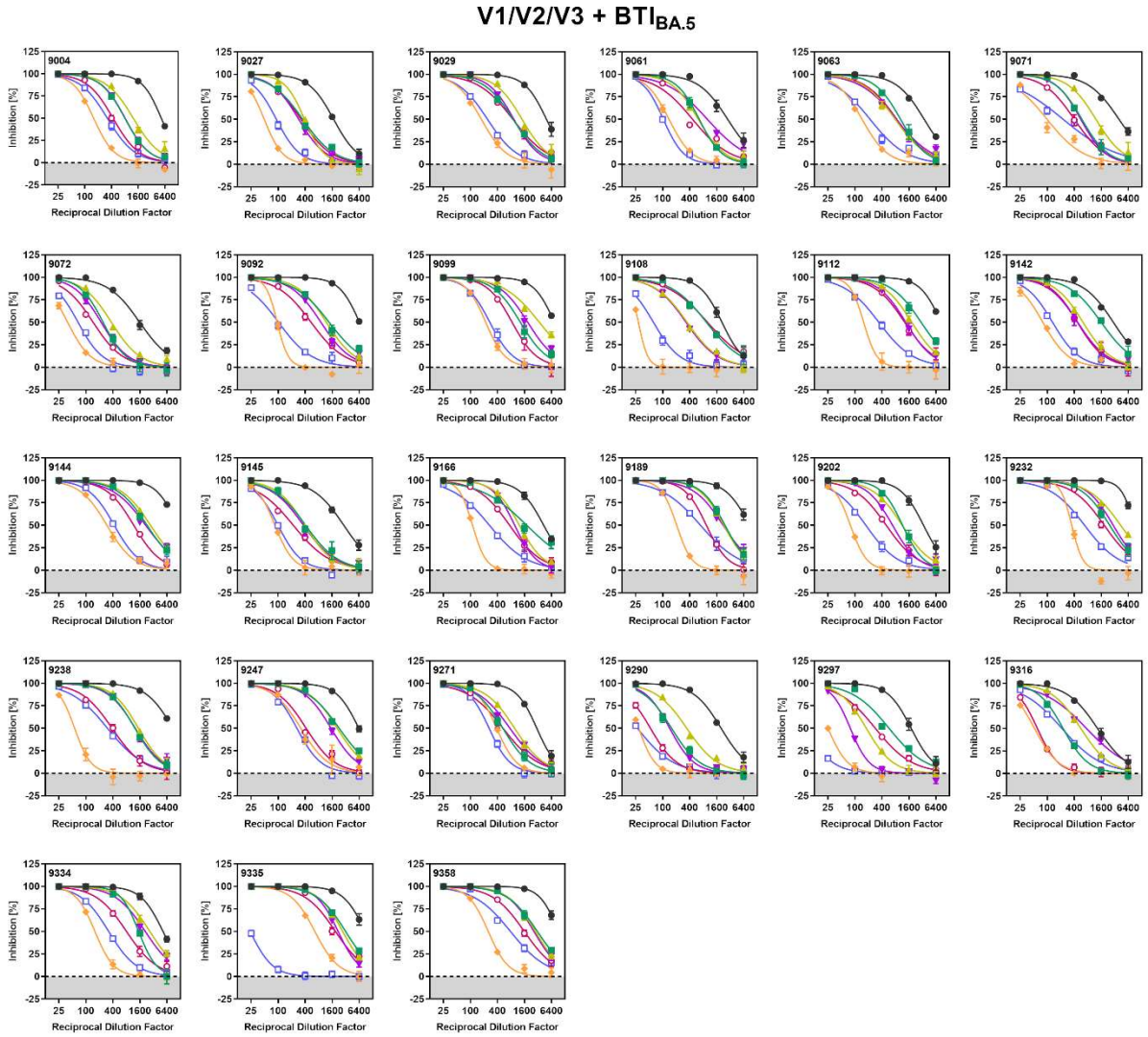

Figure S7: Individual neutralisation data for cohort V1/V2/V3 + BTI$_{BA.5}$.

Plasma-specific neutralisation data for SARS-CoV-2 lineages B.1 (dark grey), BA.1 (green), BA.4-5 (yellow), BA.4.6 (purple), BA.2.75.2 (orange), BJ.1 (pink), and BQ.1.1 (blue).

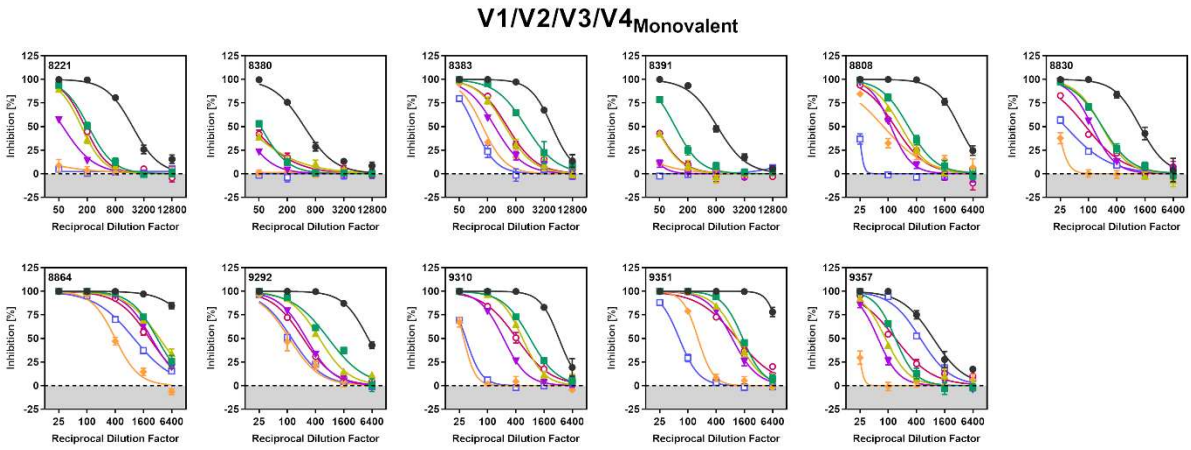

Figure S8: Individual neutralisation data for cohort V1/V2/V3/V4$_{Monovalent}$.

Plasma-specific neutralisation data for SARS-CoV-2 lineages B.1 (dark grey), BA.1 (green), BA.4-5 (yellow), BA.4.6 (purple), BA.2.75.2 (orange), BJ.1 (pink), and BQ.1.1 (blue).

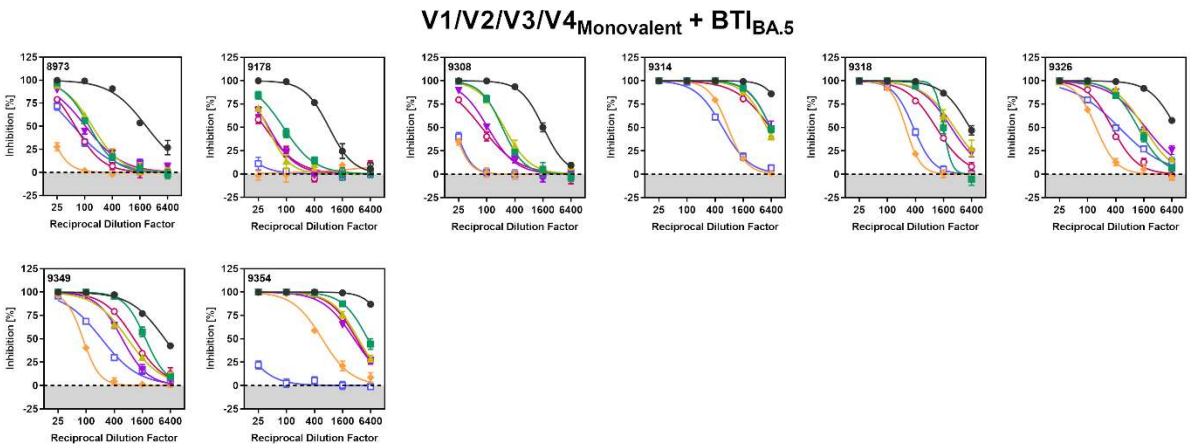

Figure S9: Individual neutralisation data for cohort V1/V2/V3/V4$_{Monovalent}$ + BTI$_{BA.5}$.

Plasma-specific neutralisation data for SARS-CoV-2 lineages B.1 (dark grey), BA.1 (green), BA.4-5 (yellow), BA.4.6 (purple), BA.2.75.2 (orange), BJ.1 (pink), and BQ.1.1 (blue).

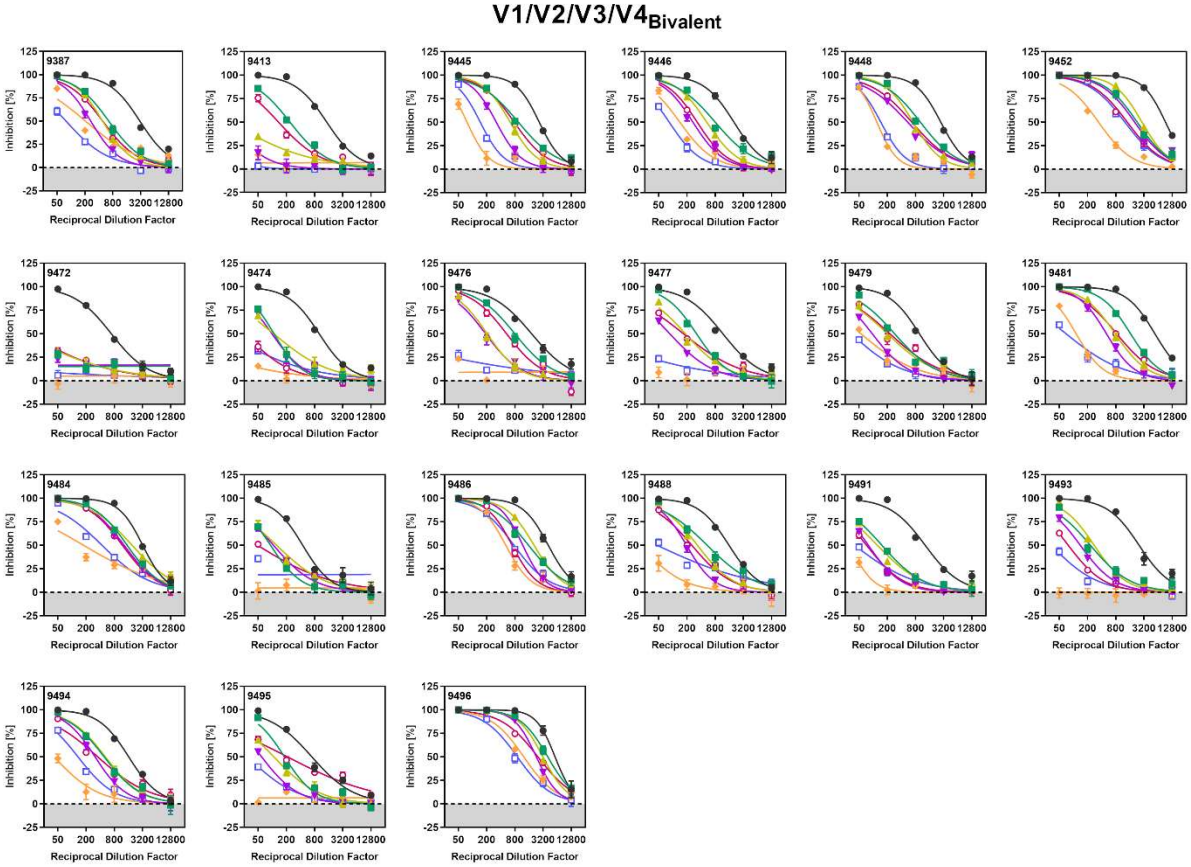

Figure S10: Individual neutralisation data for cohort V1/V2/V3/V4$_{Bivalent}$.

Plasma-specific neutralisation data for SARS-CoV-2 lineages B.1 (dark grey), BA.1 (green), BA.4-5 (yellow), BA.4.6 (purple), BA.2.75.2 (orange), BJ.1 (pink), and BQ.1.1 (blue).

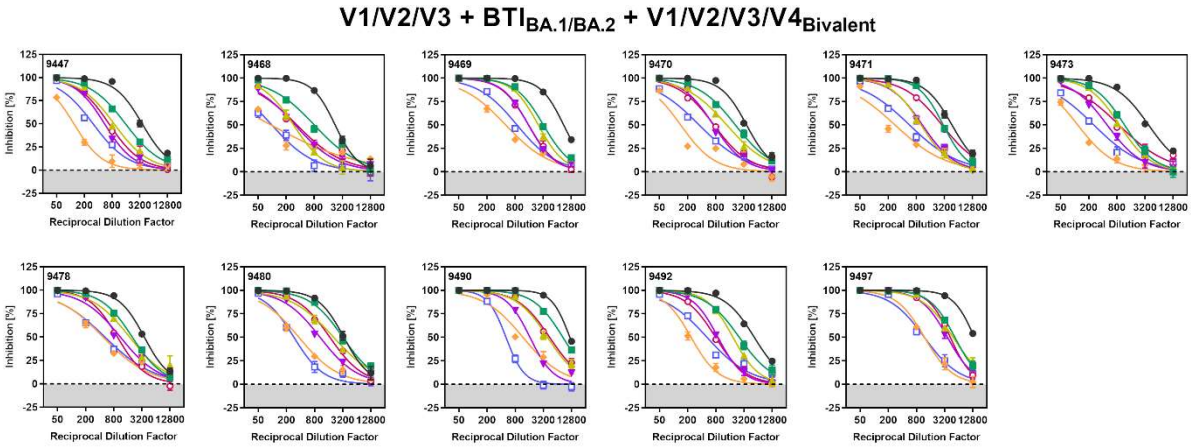

Figure S11: Individual neutralisation data for cohort V1/V2/V3 + BTI$_{BA.5}$ + V4$_{Bivalent}$.

Plasma-specific neutralisation data for SARS-CoV-2 lineages B.1 (dark grey), BA.1 (green), BA.4-5 (yellow), BA.4.6 (purple), BA.2.75.2 (orange), BJ.1 (pink), and BQ.1.1 (blue).